

# A FINITE-ELEMENT ANALYSIS OF ELECTROMAGNETIC SHEET METAL-EXPANSION PROCESS<sup>①</sup>

Huang Shangyu, Chang Zhihua, Wang Zhongren<sup>†</sup>, Wang Lifeng and Yang Mei

*School of Materials Engineering,*

*Wuhan Automotive Polytechnic University, Wuhan 430070, P. R. China*

<sup>†</sup>*School of Materials Science and Engineering, Harbin Institute of Technology,*

*Harbin 150006, P. R. China*

**ABSTRACT** Sheet metal working by a flat spiral coil, a typical way of electromagnetic forming, has been extensively applied in the practical production. Based on the equivalent electric circuit method for analyzing the discharging process and the numerical model of magnetic pressure, an analysis of the effects of the force-energy parameters on the forming process in sheet metal expansion was made by the dynamic incremental non-linear elastoplastic finite element method. The expansion height varies with the force-energy parameters of the electromagnetic forming system by experimental analysis, but the deforming speed becomes larger and the forming time shortens as the voltage or capacitance increases, which is just the reversal of the inductance. The experimental results showed that the scheme of the present analysis is valid for the prediction of the final shape in electromagnetic forming of flat workpiece. However, in order to obtain a more realistic description of the dynamic deformation fields, some improvement should be made in air damping model.

**Key words** finite element analysis electromagnetic forming magnetic pressure

## 1 INTRODUCTION

Electromagnetic forming, essentially being a kind of application of impulse intensive current technique in metal working, deals with many subjects such as electricity, electromagnetism, electrodynamics, plastic dynamics, mechanical and materials science and so on. Because of the complexity of electromagnetism and electrodynamics as well as the imperfection of plastic dynamics, especially the interaction of discharging and deforming processes, it is fairly difficult to systematically investigate the electromagnetic forming process by a single experiment means, and so far there still exist many key issues in this field which should be studied.

With the development of computer technique, non-linear continuous medium mechanics and finite element method, more attentions have been paid to the numerical simulation of electromagnetic forming processes. In the middle age of

the 1980's, Suzuki *et al*<sup>[1]</sup> performed the finite element analysis of tube expansion under an assumed magnetic pressure distribution. After that, Murata *et al*<sup>[2]</sup> applied the finite element method to the analysis of direct electrode contact tube expansion, Min *et al*<sup>[3]</sup> simulated the electromagnetic tube compression process by measuring the magnetic pressure, and a finite element analysis of the electromagnetic field was successfully used by Lee *et al*<sup>[4]</sup> to obtain a more realistic pressure distribution in tube expansion. However, the amount of research carried out into this process left much to be desired and little of them dealt with complex parts and compound processes, especially with electromagnetic forming of flat workpiece.

Recently, the present authors<sup>[5]</sup> developed an equivalent circuit analysis of the electromagnetic sheet breakdown metal forming, and obtained a more realistic magnetic pressure distribution. In this work, the analysis has been ex-

① Received Dec. 12, 1997; accepted Feb. 27, 1998

tended to the computer simulation of the dynamic deformation and the investigation of the effects of the force-energy parameters on the forming process in sheet metal expansion.

## 2 EXPERIMENTAL DEVICES AND MAGNETIC PRESSURE DISTRIBUTION

Experiments were made on a self-developed WG-1 electromagnetic forming machine( 10 kJ) . The device is illustrated in Fig. 1. The forming coil was wound by copper wire with rectangle section(the parameters of structure and properties are shown in Table 1); Experimental material is industrially pure aluminum ( Al 1060, thickness: 0.4 mm), its properties are given in Table 2.

**Table 1** Parameters of coil

$\rho_0$ / mm	Turn -to-turn spacing / mm	Radial width / mm	Thickness / mm	Turns	Conduc- tivity / ( $\Omega \cdot m$ ) <sup>-1</sup>
8.45	0.94	3.7	5.42	8	$6.25 \times 10^7$

The magnetic pressure exerted on the workpiece's surface is calculated from the following equation<sup>[8]</sup>:

$$\mathbf{P} = \frac{1}{\mu_0} [ \mathbf{B}_z ( \mathbf{B}_z \cdot \mathbf{n} ) - \frac{1}{2} \mathbf{B}_z^2 \mathbf{n} ] \quad (1)$$

where  $\mu_0$  is the permeability (  $H \cdot m^{-1}$  ) of vacuum,  $\mathbf{B}_z$  is the magnetic flux density ( T ) on the workpiece's surface,  $\mathbf{n}$  is the outward normal unit vector on the surface subjected to pressure and  $\mathbf{P}$  is Maxwell's stress tensor which is equivalent to the magnetic pressure. In simplification, Eqn. ( 1 ) can be rewritten as

$$P = \frac{(B_r + B'_r)^2}{2\mu_0} \quad (2)$$

where  $B_r$  and  $B'_r$  are the radial components of the magnetic flux density respectively produced by forming coil and workpiece, their expressions are in the Reference[ 5 ].

The magnetic pressure distribution is shown in Fig. 2.

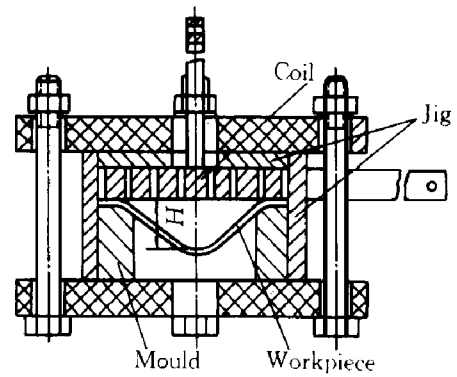


**Fig. 1** Sketch of experimental device

## 3 FINITE-ELEMENT ANALYSIS MODEL

Magnetic impulsive bulging of flat workpiece is a dynamic and high-speed response process. It can be analyzed by dynamic incremental non-linear elastoplastic finite element method. One-twelfth of the workpiece was considered in the analysis because of the axisymmetry of deformation( as shown in Fig. 3(a) ).

Triangle sheet/ shell elements were used for the element partitions of the workpiece and 4 node elements for the die corner. In consideration of the nonuniform of magnetic pressure in radial direction( shown in Fig. 2( a) ), the radius was divided into 30 equal sections and the circumferences were divided into sections of  $\pi/30$ ,  $\pi/15$ ,  $\pi/10$ ,  $2\pi/15$  and  $\pi/6$ ( as shown in Fig. 3( a) ); mould was divided into 4 equal parts( as shown in Fig. 3( b) ). The magnetic pressure at each node can be calculated by Eqn. ( 2 ), then the distributed pressure acting on each element can be obtained by interpolation. The workpieces were considered as isotropic elastoplastic material and the mould was considered as rigid bodies, strain rate effects were neglected in the computation.

**Table 2** Material properties of Al 1060<sup>[2, 6, 7]</sup>

Hardening modulus/ MPa	Hardening exponent	Yield stress / MPa	Poisson's ratio	Young's modulus / GPa	Density / ( $kg \cdot m^{-3}$ )	Conductivity / ( $\Omega \cdot m$ ) <sup>-1</sup>
140	0.32	36.3	0.33	72.5	2699.0	$3.8 \times 10^7$

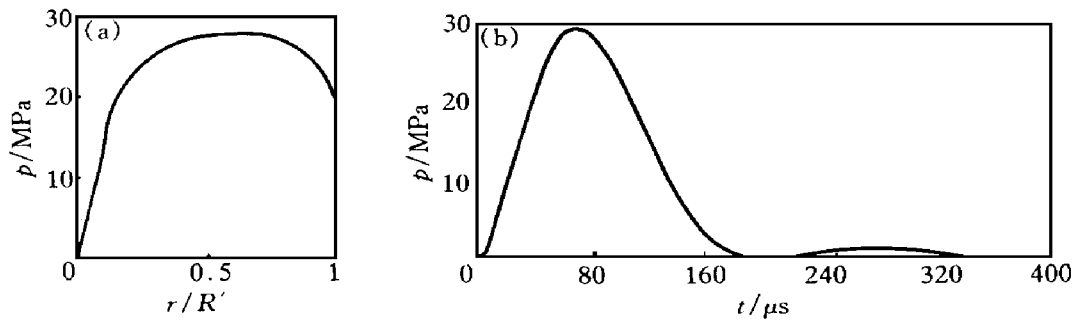


**Fig. 2** Distribution of magnetic pressure

( $d_0 = 1 \text{ mm}$ ,  $V = 3 \text{ kV}$ ,  $C = 390 \text{ } \mu\text{F}$ ,  $L = 8.4 \text{ } \mu\text{H}$ ,  $R' = 27 \text{ mm}$ )

(a) —Radial distribution,  $t = \pi/2\omega$ ; (b) —Time characteristic,  $r/R' = 0.5$

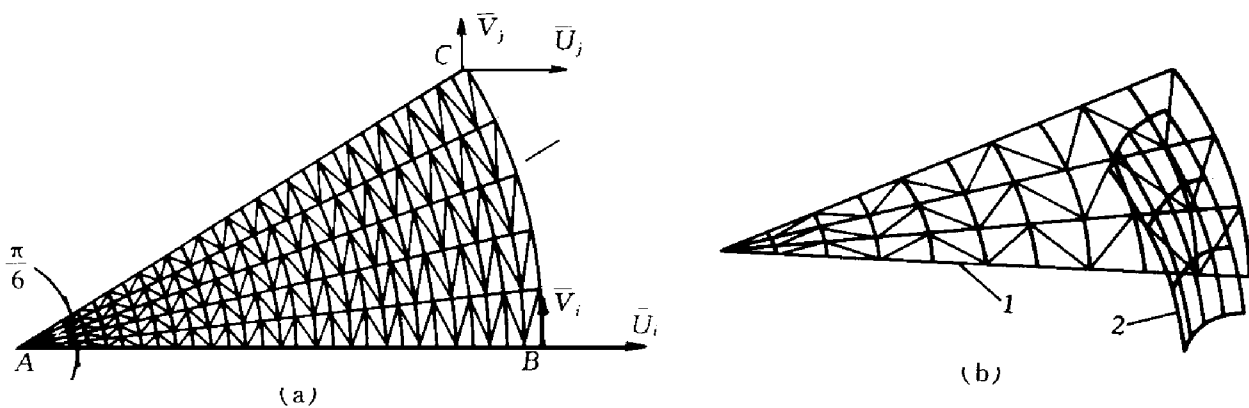


**Fig. 3** Element partitions of FEM model

(a) —Element partions of workpiece; (b) —Discription of contact surface

1—Driving contact surface (Blank); 2—Passive contact surface (Edge of mould)

At any angle, the displacement meets periodic conditions and the boundary of the flat workpiece is fixed by mould, which consults in following constraint equations:

$$\begin{cases} \bar{V}_i = 0, (AB) \\ \bar{V}_j = \bar{U}_j \cdot \tan \frac{\pi}{6}, (AC) \\ \bar{U} = \bar{V} = 0, (A) \\ \bar{U} = \bar{V} = \bar{W} = 0, (BC) \end{cases} \quad (3)$$

where  $\bar{U}$ ,  $\bar{V}$  and  $\bar{W}$  are the displacement in the  $x$ ,  $y$  and  $z$  direction respectively.

The structural damping of the workpiece should be neglected for the small mass, medium damping is directly proportional to the deforming velocity<sup>[9]</sup>. Since low frequency plays a leading role in forming process<sup>[10]</sup>, it can be suggested that damping matrix be written as

$$\mathbf{D} = \gamma \cdot \mathbf{U}_0 \mathbf{M} \quad (4)$$

where  $\mathbf{U}_0$  is the sonic speed and  $\mathbf{M}$  is the global

mass matrix.

To insure accuracy, time increment was set as<sup>[2]</sup>:  $\Delta t = \pi / (250\omega)$ .

## 4 ANALYSIS OF SIMULATING RESULTS

Fig. 4 shows the computation results of dynamic deformation field for flat workpiece bulging. From Fig. 4(a) it is known that the prediction of final shape is consistent with the experimental result. During the course of loading, the workpiece shows little deformation and it deforms mainly after impulsive load had disappeared, which indicates that the inertial force plays a leading role in magnetic impulsive forming process for flat workpiece. Only the minority of the work done by magnetic pressure transforms into plastic deformation energy, while the majority turns into the motive energy. After load drops to zero, the motive energy then transforms

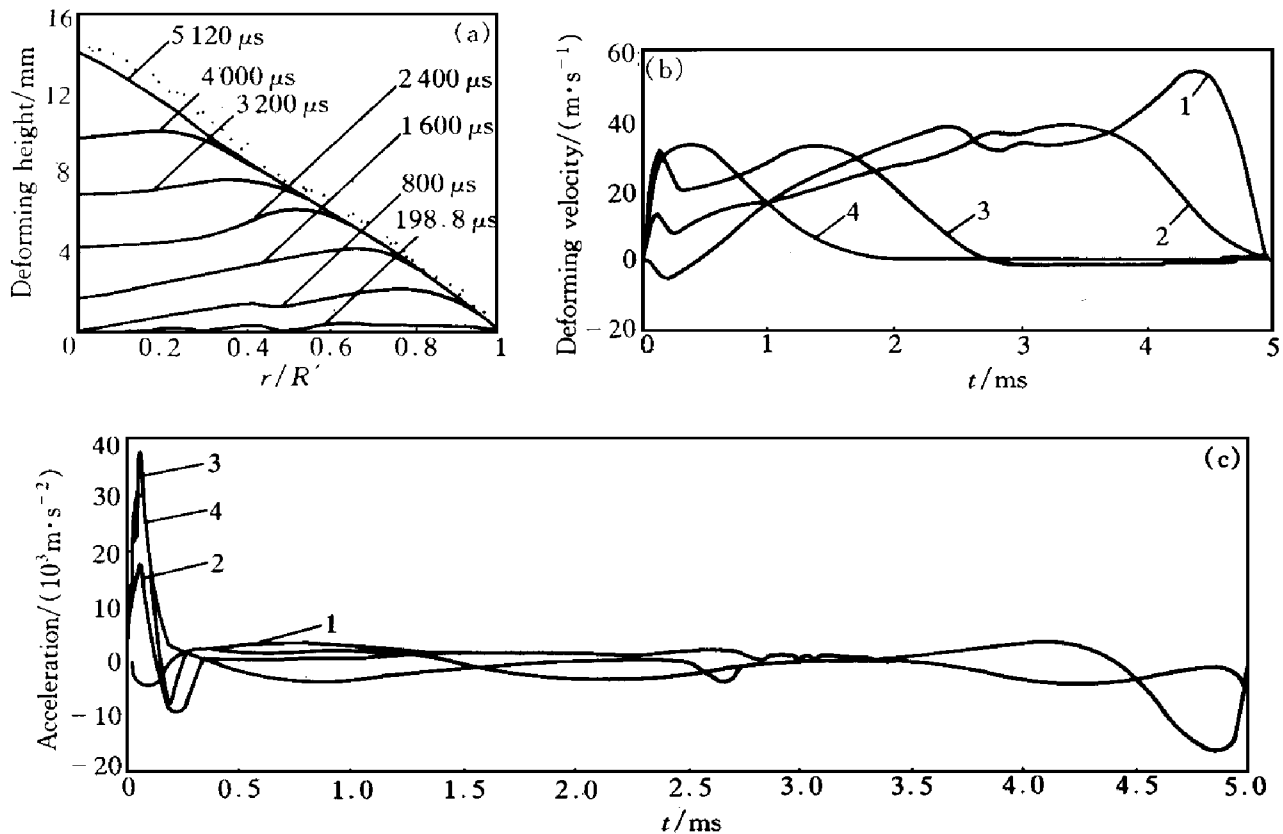


**Fig. 4** Deformation field of sheet aluminum during free electromagnetic bulging  
( $d_0 = 1 \text{ mm}$ ,  $V = 3 \text{ kV}$ ,  $C = 390 \text{ } \mu\text{F}$ ,  $L = 8.4 \text{ } \mu\text{H}$ ,  $R' = 27 \text{ mm}$ )

Solid line — Calculated value; Dotted line — Measured value.

(a) — Displacement field; (b) — Axial velocity field; (c) — Axial acceleration field

1 — Velocity and acceleration of center point;

2, 3 and 4 — Velocity and acceleration of points at  $1/4$ ,  $1/2$  and  $3/4$  radius

into plastic deformation energy to realize the forming of workpiece. The effects of forming process on discharging process can be neglected in load computation because of the little deformation of workpiece during the acting period of magnetic pressure, which is different from the electromagnetic tube expansion<sup>[11, 12]</sup>. The dynamic shape of workpiece at every moment during forming process is similar to the measurement results of the Reference[13], but there exists a time lag to some extent.

In the deformation zone, the axial motive velocity and initial moment of different point are distinctive (Fig. 4(b)). The part nearby  $1/2$  radius moves firstly because of the maximum magnetic pressure (shown in Fig. 2(a)) and the center part of the workpiece, almost driven by surroundings, moves later because of the minimum pressures. In initial forming stage, it is for the

inertia (Motion of surrounding particles drive the central point to deform, while inertia makes it in the initial stationary state) that the velocity of center part become negative; in later forming period, the velocity, driven by surroundings, gets to the maximum. The ending of deformation postpones along the entry of the mould to the center of the workpiece, which is consistent with the experimental results of the References [14], however, the calculated amplitude of velocity is smaller and the error is a bit larger.

Axial acceleration field is complex (as shown in Fig. 4(c)), which is produced by the magnetic pressures and the inertial force. During loading stage, maximum and minimum value of acceleration synchronize with that of the magnetic pressure, except a minor part near the center. The negative acceleration is also caused by inertia.

Fig. 5 shows the simulation results of the final shape and the velocity field at the center of workpiece in different electrical parameters (voltage, capacity and inductance). It can be inferred from the diagram that the forming processes and deformation degree are closely related to the electrical parameters. With the other parameters remain constant, as the voltage or capacity increases, the forming speed rises obviously, the deformation ends earlier and the bulging height be-

come larger, which is for the increase in discharging energy ( $cv^2/2$ ); as the inductance increases, if the discharging energy remains constant, the forming speed, the deformation time and the bulging height vary in the opposite direction, while a part of energy is consumed by the increment of the inductance, the discharging current decreases and the magnetic pressure is correspondingly reduced.

In summary, except for the error of form-

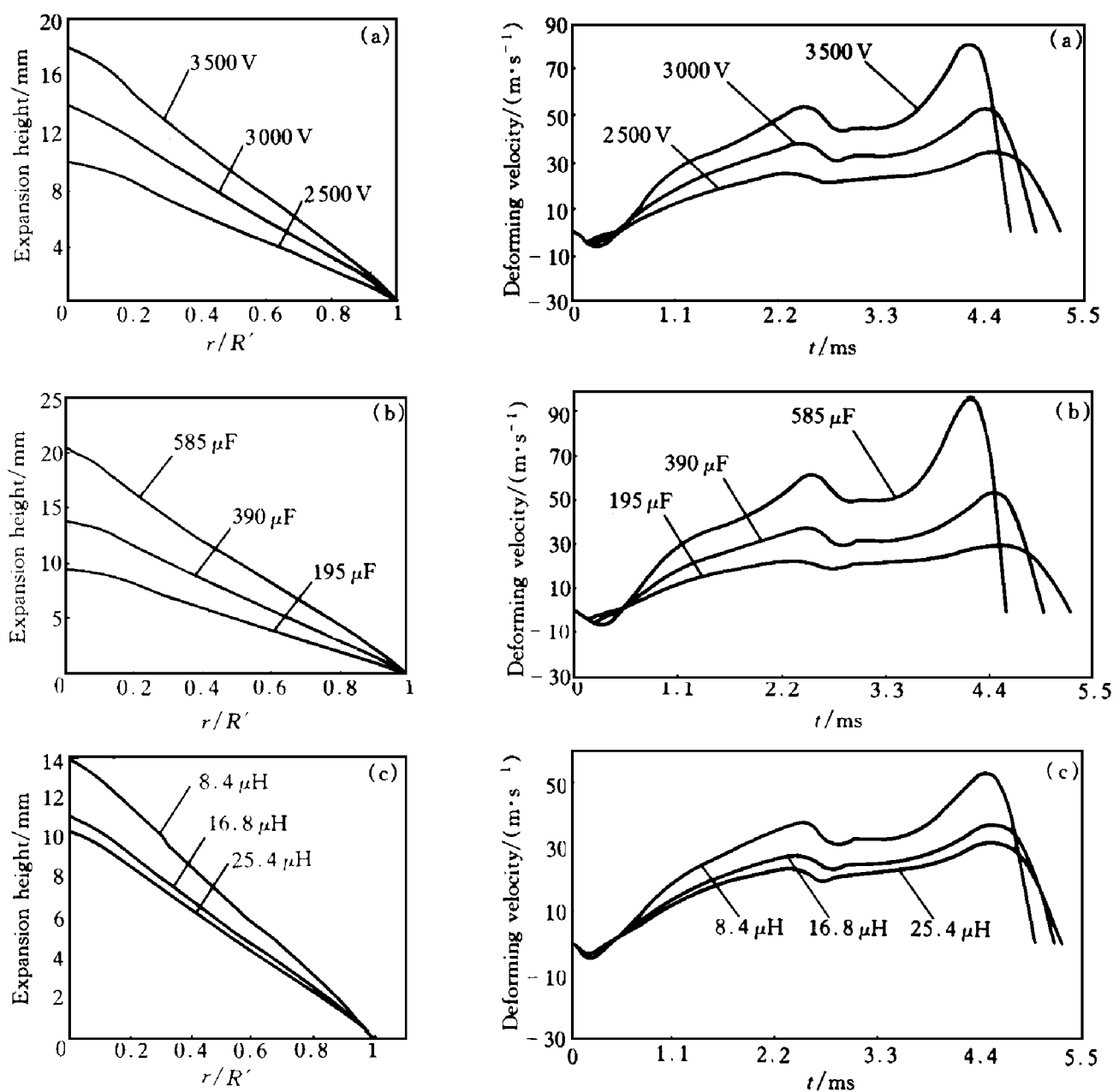


**Fig. 5** Free bulging processes of sheet aluminum in different electrical parameters  
 (a) —Different voltage(  $C = 390 \mu\text{F}$ ,  $L = 8.4 \mu\text{H}$ ); (b) —Different capacity(  $V = 3 \text{ kV}$ ,  $L = 8.4 \mu\text{H}$ );  
 (c) —Different inductance(  $V = 3 \text{ kV}$ ,  $C = 390 \mu\text{F}$ )

ing speed in magnitude and of deformation time, the results of simulation are in accordance with the actual shape of workpiece and those of related experiments. Because the final shape of the analysis and of the experiments show good agreement, it can be deduced that the corresponding relations (including place, time and magnitude) of simulated deformation field are identical with those of actual forming processes, though reduction in magnitude of velocity field in the same scale has resulted in the prolongation of deforming course. For the above reasons, the present authors infer that deforming lag and certain error of velocity magnitude are mainly caused by the only consideration of low frequency in the calculating damping matrix, and the simplification of flat spiral coil may also bring about a little calculating error.

## 5 CONCLUSIONS

(1) The inertial force plays a leading role in magnetic impulsive forming for flat workpiece. In consideration of little deformation during loading stage, the interaction of discharging and forming process can be neglected.

(2) During loading stage, except a minor part surrounding the center of the workpiece, the maximum and minimum value of deforming acceleration synchronize with those of the magnetic pressure.

(3) Neglection of high frequency in damping matrix can lead to certain calculating error in the analysis of deforming time and velocity magnitude, but it doesn't change the corresponding relation in the place, time and magnitude of deformation field, and so, is useful in the prediction of workpiece's final shape.

(4) For non-strain-rate sensitive materials, the static constitutive equations are still applicable to the analysis of high-speed forming process by using elastoplastic finite element method.

(5) As voltage or capacity increases, the forming speed rises obviously and the deformation ends more earlier; as the discharging energy

remains constant and the inductance increases, the forming speed and the deformation time respectively vary in the opposite direction.

## ACKNOWLEDGEMENT

Most of this work has been made possible by an open research foundation of State Key Lab. of Plastic Forming Simulation & Die Technology, 96-2.

## REFERENCES

- 1 Suzuki H *et al.* In: The Organizing Committee of the First International Conference on Technology of Plasticity eds. Advanced Technology of Plasticity, Vol 1. Tokyo: The Japan Society for Technology of Plasticity and the Japan Society of Precision Engineering, 1984: 367- 372.
- 2 Murata M *et al.* In: Wang Yungan, Zhou Shineng, Li Congxin eds. Proc Int Conf on Advanced Technology and Machinery in Metal forming. Wuhan: Huazhong University of Science and Technology Press, 1992: 216- 229.
- 3 Min Dong-Kyun *et al.* Journal of Materials Processing Technology, 1993, 38(1): 29- 40.
- 4 Lee Sung-Ho *et al.* ASME J Eng Mater Technol, 1994, 116: 250.
- 5 Huang Shangyu *et al.* The Chinese Journal of Non-ferrous Metals, (in Chinese), 1998, 8(3).
- 6 Wang Xiaopei. A Handbook of Stamping, (in Chinese). Beijing: Mechanical Industry Press, 1990: 503.
- 7 Liang Chanbin. Electromagnetism, (in Chinese). Beijing: People's Educational Publisher, 1980: 191.
- 8 Durney C H and Johnson C C. Introduction to Modern Electromagnetics. New York: McGraw-Hill, 1969: 163.
- 9 Yang Guitong. Plastic Dynamics, (in Chinese). Beijing: Tsinghua University Press, 1984: 269.
- 10 Wu Yongguo. Journal of Plasticity Engineering, (in Chinese), 1995, 2(3): 31- 36.
- 11 Negishi H *et al.* Journal of JSTP, (in Japanese), 1980, 21(234): 642- 648.
- 12 Zhang Shoubin. PhD thesis, (in Chinese). Harbin: Harbin Institute of Technology, 1990: 46- 54.
- 13 Negishi H *et al.* Journal of JSTP, (in Japanese), 1977, 18(194): 197- 203.
- 14 Popovider E A. Forging & Stamping Production, (In Russian), 1984, (7): 2- 9.

(Edited by Yuan Saiqian)